

# Transannular $\pi$ – $\pi$ interactions in janusenes and in related rigid systems with cofacial aromatic rings; gauging aromaticity in the hydrocarbons and in model carbocations; a DFT study†

Takao Okazaki<sup>a,b</sup> and Kenneth K. Laali<sup>\*a</sup>

Received 28th April 2006, Accepted 16th June 2006

First published as an Advance Article on the web 14th July 2006

DOI: 10.1039/b606070f

The utility of NICS (nuclear independent chemical shift) as a probe for detecting/sensing variation in aromaticity due to transannular  $\pi$ – $\pi$  interactions in janusene **2**, a [3.3]orthocyclophane having two cofacial benzene rings within van der Waals distance, its tetrafluoro- and octafluoro-derivatives **4** and **5**, and in tropiliojanusene **6** was studied by DFT at the B3LYP/6-31G(d) level. The related hydrocarbons **8** and **8a** with a buried double-bond and their carbocations were also included in this study. Whereas NICS(0) and NICS(1) are rather insensitive to transannular interactions, computed NICS(1)<sub>zz</sub> values are larger and more negative for both  $\pi$ -decks in the interannular space and this is consistent with increased transannular  $\pi$ – $\pi$  interactions in the cofacial rings, previously shown in these systems *via* spectroscopic studies (UV and NMR), and by electrophilic chemistry. Transannular effects in **2**, **4**, and **6** were also probed by examining the forms of HOMO–LUMOs. Attempts to measure donor–accepter interactions between electron rich/electron poor cofacial decks *via* NICS(1)<sub>zz</sub> through substituent effects proved unsuccessful, resulting in only very small changes. Protonation of the double-bond buried in between the two  $\pi$ -decks in **8** and **8a** results in internally  $\pi$ -stabilized carbocations that exhibit more negative NICS(1) and NICS(1)<sub>zz</sub> values in the interannular space. GIAO NMR data were computed for the neutral hydrocarbons and their derived carbocations, as a guiding tool for planned experimental studies.

## Introduction

Since its introduction a decade ago by Schleyer,<sup>1</sup> nucleus independent chemical shift NICS has been successfully applied to a wide variety of neutral and charged structures, namely annulenes,<sup>2</sup> heterocycles,<sup>3</sup> metal  $\pi$ -complexes,<sup>4</sup> strained cage compounds with 4-membered rings,<sup>5</sup> benzyl cations,<sup>6</sup> carbocations, dications, and dianions from nonalternant-PAHs,<sup>7</sup> and anti-aromatic dications.<sup>8</sup> NICS has also been applied to probe homoaromaticity,<sup>9</sup> local aromaticity in large polynuclear aromatic hydrocarbons,<sup>10</sup> spherical aromaticity in fullerenes,<sup>11</sup> and to examine transition states in cycloadditions.<sup>12</sup>

Later it was shown<sup>13</sup> that NICS(1) is more suitable than NICS(0) as an aromaticity index because of diminished local contributions to the ring current effects, and that NICS<sub>zz</sub> (principal axis perpendicular to the ring plane) can provide a more accurate analysis of aromaticity in the  $\pi$ -system of annulenes relative to isotropic NICS parameters due to the fact that NICS<sub>zz</sub> is dominated by contribution from the  $\pi$ -system, whereas NICS(0) contains sigma bond contribution.<sup>14</sup> In a recent report, Sola

*et al.*<sup>15a</sup> examined local aromaticity in a series of PAHs, namely [*n*]acenes and [*n*]phenacenes and in representative [*n*]helicenes *via* electronic (PDI), geometric (HOMA) and magnetic (NICS) criteria. With [*n*]helicenes (*n* = 6–9) computed local aromaticity in the terminal rings was larger than expected and this was attributed to magnetic coupling of cofacial rings. Model studies with naphthalene and phenanthrene “sandwiches” showed that NICS is artificially augmented as a function of distance between the opposite decks.<sup>15a</sup> Efficacy of the PDI and HOMA methods in comparison with NICS was examined in a recent review by Sola and associates.<sup>15b</sup> At about the same time, we reported a DFT study focusing on the geometries, strain energies and conformations in [2.2]cyclophanes, and applied NICS and HOMA to explore their aromaticity.<sup>16</sup> Computed NICS values implied an increase in electron density inside the rings as a result of stacking effect and a further increase *via* the bridging process. Moreover NICS<sub>zz</sub> indicated that predominant increase in electron density occurs in the interannular space, *i.e.* in the cavity of the molecule. In an independent earlier study, Salcedo and associates<sup>17</sup> used DFT to address aromaticity and transannular effects in representative substituted [2.2]paracyclophanes and also reported NICS(0) values for the  $\pi$ -deck. Substitution in one deck led to small changes in NICS(0) of the opposite deck. With R = OH, NICS(0) implied activation of the opposite deck (more negative value) but surprisingly, the trend was the same with R = CN or NO<sub>2</sub>, implying the opposite deck was activated.<sup>17</sup> An earlier report by the same group examined aromaticity in representative superphanes.<sup>18</sup> Transannular effects were implied by computing the HOMO–LUMO forms. An interesting finding was that the

<sup>a</sup>Department of Chemistry, Kent State University, Kent, OH 44242. E-mail: klaali@kent.edu; Fax: 330-6723816; Tel: 330-6722988

<sup>b</sup>Department of Energy and Hydrocarbon Chemistry, Kyoto University, Kyoto, Japan

† Electronic supplementary information (ESI) available: Fig. S1–S14 and Tables S1–S5. See DOI: 10.1039/b606070f

‡ For a recent authoritative progress review/compilation see ref. 26: Z. Chen, C. S. Wannere, C. Corminboeuf, R. Puchta and P. v. R. Schleyer, *Chem. Rev.*, 2005, **105**, 3842

highly rigid [2<sub>6</sub>] (1,2,3,4,5,6) cyclophane was computed to be more aromatic by NICS(2) (center of the molecule) than by NICS(1).<sup>18</sup>

For a number of years we have been interested in structural/electronic properties and electrophilic reactivity in molecules with parallel or almost parallel  $\pi$ -faces within the van der Waals distance.<sup>19</sup> These studies centered on rigid cyclophanes namely [2.2]cyclophane **1**, janusene “JAN” **2** and their derivatives having stacked electron-rich/electron-poor  $\pi$ -decks as in tetrafluoro[2.2]paracyclophane **3**, tetrafluorojanusene “F<sub>4</sub>-JAN” **4**, octafluorojanusene “F<sub>8</sub>-JAN” **5**, and tropilijanusene “trop-JAN” **6**, as well as on the perfluorinated derivatives such as octafluoro[2.2]paracyclophane **7** (Fig. 1).<sup>19</sup>

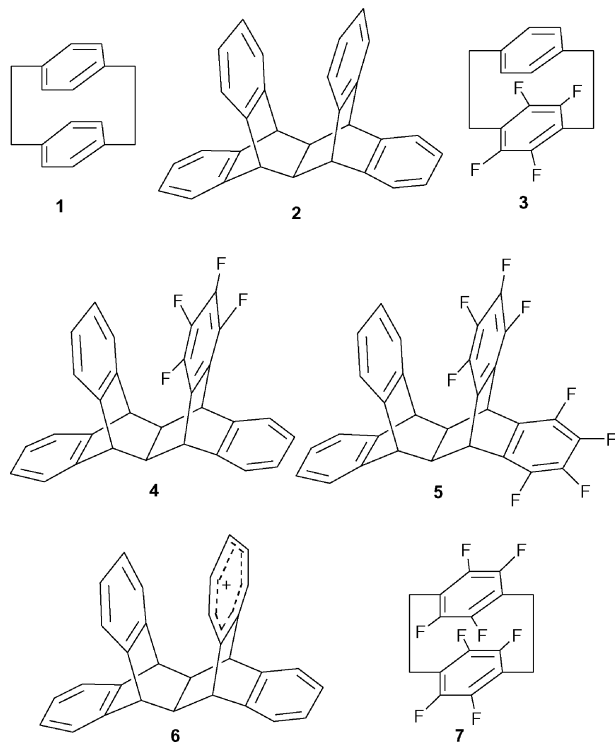


**Fig. 1** Structures of [2.2]paracyclophane (**1**), JAN (**2**), tetrafluoro[2.2]paracyclophane (**3**), F<sub>4</sub>-JAN (**4**), F<sub>8</sub>-JAN (**5**), trop-JAN (**6**), and octafluoro[2.2]paracyclophane (**7**).

Transannular deactivation in **3** is manifested in the lack of reactivity in conventional electrophilic aromatic substitution reactions such as bromination and acylation.<sup>19a,19b</sup> Transannular directive effects in [2.2]paracyclophanes were earlier demonstrated in the pioneering work of Cram.<sup>20</sup> The presence of attractive transannular donor–acceptor interaction in **3** was inferred from its UV spectrum.<sup>19a</sup> NMR studies of **3H<sup>+</sup>** and **7H<sup>+</sup>** showed that the cofacial arenium ions were shielded by the opposite deck, demonstrating that the direction of transannular shielding is reversed/switched in the carbocations (Fig. 2).<sup>19a</sup> Whereas **3H<sup>+</sup>** is directly observable under stable ion conditions, attempted ring protonation of **4** resulted in broad resonances (with concomitant generation of radical cation);<sup>19b</sup> these features were attributed to rapid 1,2-hydride shifts and interannular proton transfer.<sup>19d</sup>

In light of these earlier reports and in continuation of our interest in transannular electrophilic reactivity in cyclophanes, and in persistent carbocations derived from cyclophanes, we report

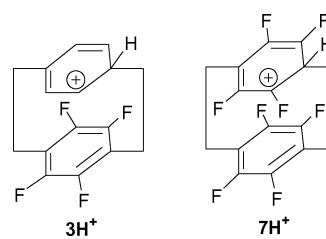


**Fig. 2** Persistent carbocations derived from **3** and **7**.

here a DFT study, emphasizing the janusene skeleton and its carbocations. NICS(0), NICS(1), NICS<sub>zz</sub> and NICS (at center) were applied to explore the sensitivity of these methods to changes in aromaticity *via* transannular effects. For comparison, transannular effects were also gauged by examining the HOMO/LUMO forms and by calculating energy gaps. In addition, NICS data were computed for a series of substituted janusenes, to test the response of the method to changes in aromaticity *via* transannular substituent effects. For comparative purposes, GIAO-NMR data were computed for several neutral janusenes. Finally, relative energies and GIAO-NMR data were also computed for the carbocations derived from the “entombed olefins” **8** and **8a** (Fig. 3).

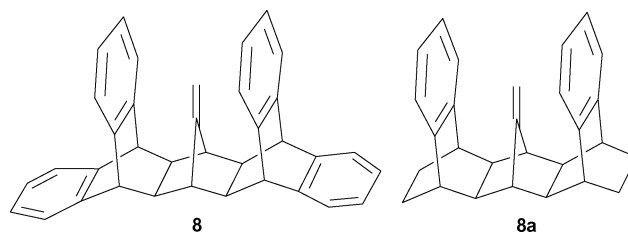


**Fig. 3** 5,14;7,12-bis(*o*-benzo)-6,13-ethenylidene-5,5a,6,6a,7,12,12a,13,13a,14-decahydropentacene (**8**) and related compound **8a**.

## Results and discussion

### Computational protocols

Structures were optimized using molecular point groups shown in Tables S1–S5† by the density functional theory (DFT)<sup>21</sup> method at B3LYP/6-31G(d) level, using the Gaussian 03 package.<sup>22</sup> Computed geometries were verified to be minima with no imaginary frequency at the same level. Nuclear independent chemical shifts (NICS)<sup>1</sup> were calculated at 0 and 1 Å above the ring center, denoted as NICS(0)<sup>1</sup> and NICS(1),<sup>13</sup> by the GIAO (gauge-including atomic orbital) method<sup>23</sup> at a B3LYP/6-31G(d) level. The ring centers were defined as the simple average of Cartesian coordinates for all the sp<sup>2</sup> carbons in the ring. Planes of the rings were calculated by least-square methods using coordinates of all the sp<sup>2</sup> carbons in the ring. The “out-of-plane” components of the NICS tensors were calculated at 1 Å above the ring centers by rotating the planes of the rings orthogonal to *z*-axis, which denotes as NICS(1)<sub>zz</sub>.<sup>14</sup>

### Rationale for the choice of the models

In order to assess whether or not NICS is sensitive to variations in transannular effects on aromaticity, initial studies focused on parent JAN **2**, F<sub>4</sub>-JAN **4**, and trop-JAN **6**. At the onset, the effect of sequential fluorine substitution on aromaticity in benzene itself

was investigated. As a next step, NICS data were obtained for various building blocks of compounds **2**, **4**, and **6**.

### Stepwise fluorination in benzene

Electronic energies ( $E$ ), zero point energies ( $ZPE$ ), and Gibbs free energies ( $G$ ) for benzene and its fluorinated derivatives (Fig. 4) were calculated by B3LYP/6-31G(d). The results are summarized in Table S1† along with their molecular symmetry. Among difluorobenzene isomers, **11b** (*meta*) and among trifluorobenzenes **12c** have the lowest energies. The data accord with Bader's analysis of substituent effect in terms of alternating charges, for fluorine as a  $\sigma$  abstrator– $\pi$  donor substituent.<sup>24</sup> Isomer **13c** is more stable than other tetrafluorobenzenes. Their NICS(0), NICS(1),§ and NICS(1)<sub>zz</sub> data are shown in Fig. S1† and the NICS values are plotted against the number of fluorine atoms in fluorinated benzenes in Fig. 5. Stepwise fluorination resulted in gradual but pronounced shift to more negative NICS(0) values. The shift to more negative values became much less pronounced by employing NICS(1). Interestingly, NICS(1)<sub>zz</sub> correctly predicted the expected trend of diminished ring current effects due to change in  $\pi$ -electron density.

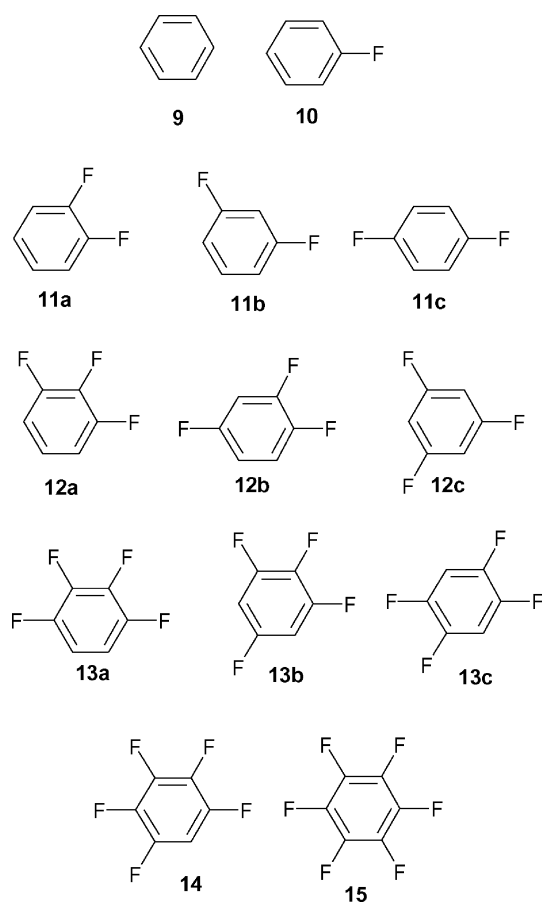


Fig. 4 Benzene (**9**) and its fluorinated derivatives **10–15**.

§ Computed NICS(0) and NICS(1) values for fluorobenzenes by B3LYP/6-311 + G\*\* were included in the recent review/compilation by Schleyer *et al.*<sup>26</sup>

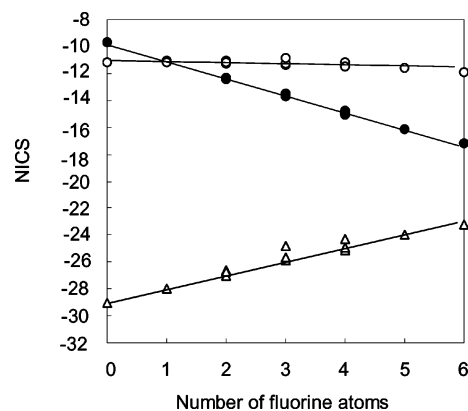


Fig. 5 Plots of NICS(0) (●), NICS(1) (○), and NICS(1)<sub>zz</sub> (△) for **9–15** versus number of fluorine atoms.

The NICS(0), NICS(1), and NICS(1)<sub>zz</sub> values correlate with the number of fluorine atoms by eqn (1)–(3). NICS(0) and NICS(1)<sub>zz</sub> increase by  $-1.26$  and  $0.98$  unit respectively per fluorine atom.

$$\text{NICS}(0) = -1.26 \times (\text{No of F atom}) - 9.8 \quad (R^2 = 0.9969) \quad (1)$$

$$\text{NICS}(1) = -0.11 \times (\text{No of F atom}) - 11.0 \quad (R^2 = 0.987) \quad (2)$$

$$\text{NICS}(1)_{zz} = 0.98 \times (\text{No of F atom}) - 28.7 \quad (R^2 = 0.947) \quad (3)$$

### Tropylium cation (**16**), bicyclo[2.2.2]octenotropylium (**17**), bicyclo[2.2.2]octenobenzene (**18**), and tetrafluorobicyclo[2.2.2]octenobenzene (**19**)

Structures **16–19** (Fig. 6) which can be viewed as building blocks/constituents of janusenes **2**, **5**, and **6** were studied next. Results of electronic energies ( $E$ ), zero point energies ( $ZPE$ ), and Gibbs free energies ( $G$ ) for these compounds along with their molecular symmetry are included in Table S2.†

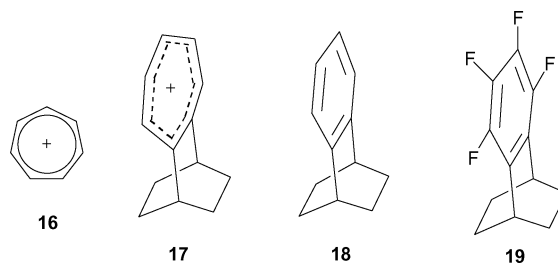
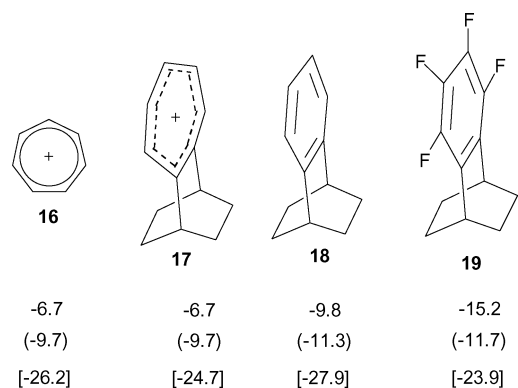


Fig. 6 Tropylium ion (**16**), bicyclo[2.2.2]octenotropylium ion (**17**), bicyclo[2.2.2]octenobenzene (**18**), and tetrafluorobicyclo[2.2.2]octenobenzene (**19**).

The NICS(0), NICS(1), and NICS(1)<sub>zz</sub> data (summarized in Fig. 7) are consistent with aromatic character.

In all cases the NICS(1)<sub>zz</sub> values are larger and more negative. There is very little difference in NICS between **16** and **17**, and between **18** and benzene. In comparing **18** and **19**, as was noted for benzene itself, only NICS(1)<sub>zz</sub> correctly predicted diminished aromaticity in the fluorinated analogs.

GIAO-derived <sup>13</sup>C NMR data for structures **16–19** (**9** and **13a** included for comparison) are summarized in Fig. S2† together with experimental data reported in the literature.



**Fig. 7** NICS(0), NICS(1) (in parenthesis), and NICS(1)<sub>zz</sub> [in brackets] for tropylium ion (**16**), bicyclo[2.2.2]octenotropylium ion (**17**), bicyclo[2.2.2]octenobenzene (**18**), and tetrafluorobicyclo[2.2.2]octenobenzene (**19**) by B3LYP/6-31G(d).

The GIAO-derived chemical shifts for **9**, **13a**, **16**, **17**, **18** and **19** are plotted against the experimental data in Fig. S3–S4.† It can be seen that the GIAO method slightly underestimates the chemical shifts (between 2–8 ppm), but the overall agreement is quite good.

**Janusene (2), tetrafluorojanusene (4), octafluorojanusene (5), tropiliojanusene (6), and syn-sesquibenzobicyclo[2.2.2]octane (20)**

Results of electronic energies (*E*), zero point energies (*ZPE*), and Gibbs free energies (*G*) for compounds **2**, **4**, **5**, **6**, and **20** (see Fig. 8) are included in Table S2† along with their molecular symmetry.

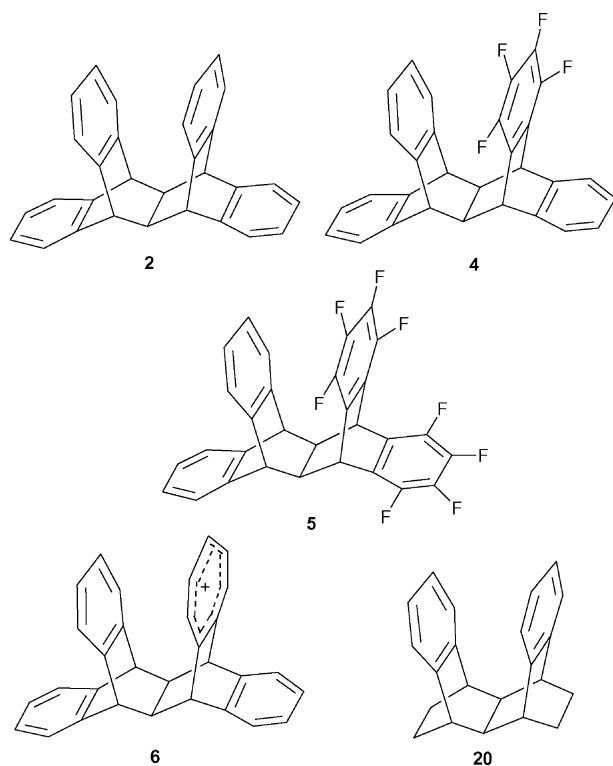


**Fig. 8** Janusene (**2**), tetrafluorojanusene (**4**), octafluorojanusene (**5**), tropiliojanusene (**6**), and *syn*-sesquibenzobicyclo[2.2.2]octane (**20**).

The NICS(0), NICS(1) and NICS(1)<sub>zz</sub> data are gathered in Fig. S5† and Fig. 9 respectively. In comparing the NICS(0) and NICS(1) data for **2** versus **20**, **19** versus **4**, and **5** relative to **19**, no noticeable changes in aromaticity due to transannular  $\pi$ – $\pi$  interactions are noted. Only in the case of **20**, NICS(1) shows a more negative value on the cofacial side of the  $\pi$ -decks. The NICS(1)<sub>zz</sub> data are more interesting and imply notable enhancement in aromatic character in **2** and **20**, for the tropylium in **6**, and for the cofacial fluorinated rings in **4** and **5**.

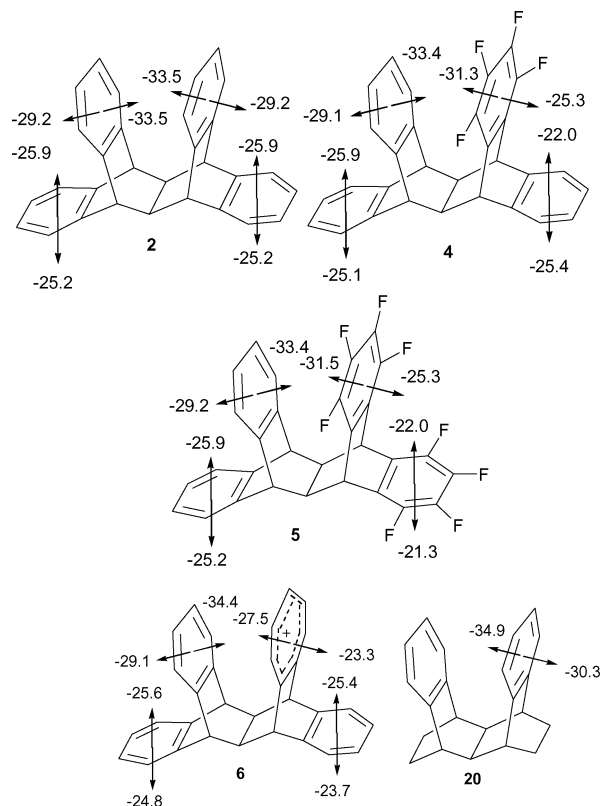


**Fig. 9** NICS(1)<sub>zz</sub> for janusenes **2**, **6**, **4**, and **5** and comparison with **20**.

The presence of favorable electron rich–electron poor  $\pi$ – $\pi$  interactions in compounds **6**, **5** and in **4** is also borne out by considering their computed HOMO–LUMO energy gaps, with **6** and **5** showing the smallest gaps (Table S3†).

A third criterion considered in the context of this study was the form of HOMO–LUMO orbitals. Fig. S6† illustrates the forms of HOMO, HOMO-1, HOMO-2 and the LUMO for **2**, **4**, **5**, and **6**. It can be seen that the LUMOs in **2**, **4**, and **5** indicate a direct interaction between cofacial rings, reflecting transannular  $\pi$ – $\pi$  overlap. A similar effect is noted in the HOMO-2 orbital in **2**. Smaller transannular interactions are implied in the LUMO and HOMO-2 orbitals in trop-JAN **6**, suggesting that transannular interactions may be less important here in reaction with nucleophile.

GIAO-derived <sup>13</sup>C NMR data are summarized in Fig. S7.† Experimental NMR data had been reported in the literature, but no detailed/specific assignments exist. GIAO-derived chemical shifts for **2**, **4**, **6**, and **20** are plotted against the experimental data in Fig. S8–S9.† The overall agreement is quite good, despite the fact that the GIAO method slightly underestimates the chemical shifts.

## Substituted janusenes with activating and deactivating groups

In the framework of this study it was relevant to explore NICS as a tool for sensing transannular substituent effects. In trop-JAN **6**, introduction of an activating substituent (OMe)

into the cofacial benzene ring could amplify transannular  $\pi$ - $\pi$  interaction (compounds **21a–21d** in Fig. 10). The presence of a strongly electron withdrawing group ( $\text{NO}_2$  and  $\text{CN}$ ) in **2** could increase electron demand transannularly (compounds **22a/22b** and **23a/23b**). Similarly, the presence of an activating group in

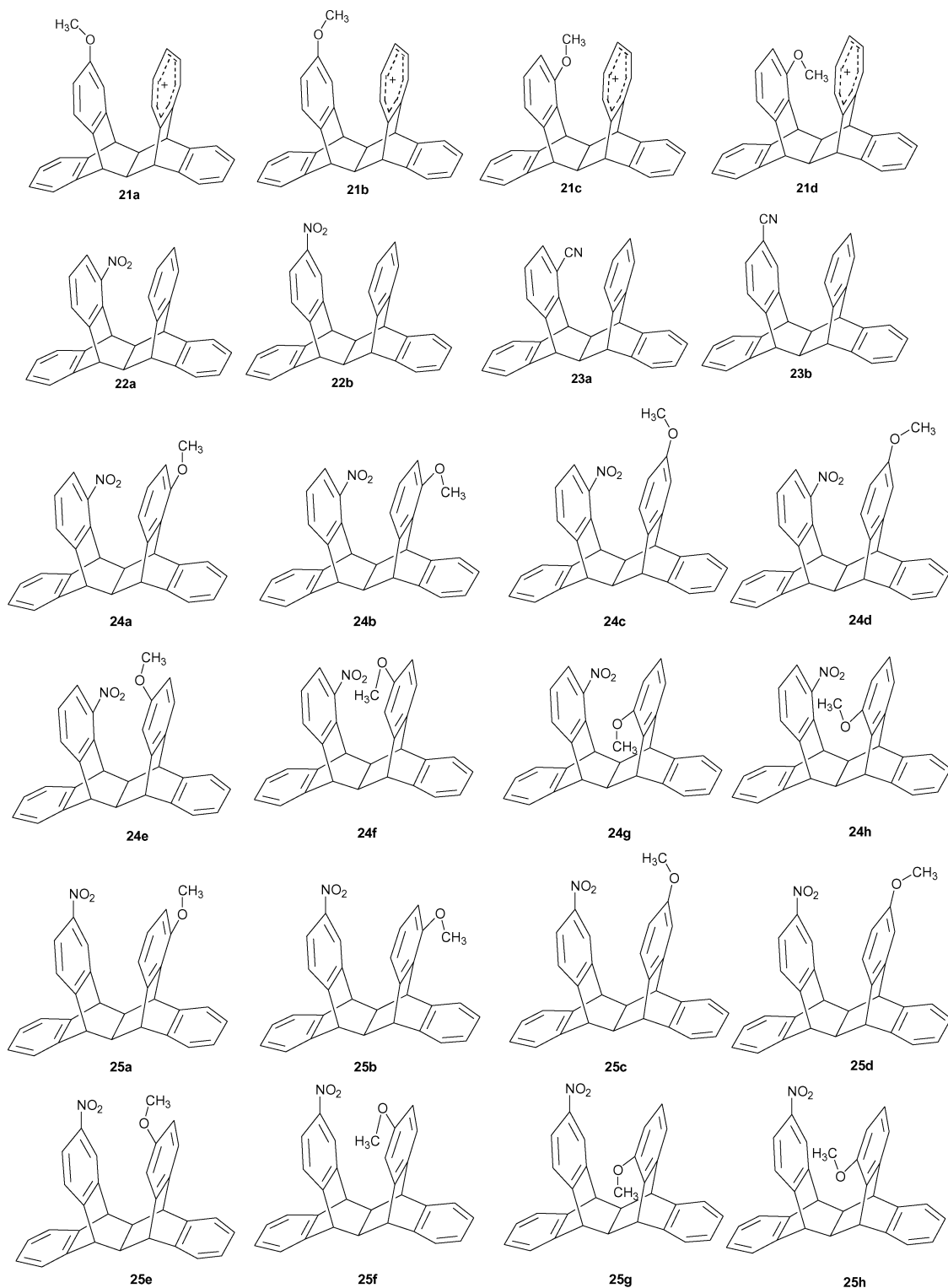


Fig. 10 Substituted janusenes **22–25** and tropiliojanusenes **21**.

one ring and a deactivating group in the other may further amplify transannular  $\pi$ - $\pi$  interactions (compounds **24a–24h**; **25a–25h**).

Results of electronic energies ( $E$ ), zero point energies ( $ZPE$ ), and Gibbs free energies ( $G$ ) for the compounds listed in Fig. 10 are

summarized in Table S4† along with their molecular symmetry. Computed NICS(1)<sub>zz</sub> and NICS at centers between two benzene rings are summarized in Figs. 11–13, and NICS(0) and NICS(1) in Fig. S10 and S11.† For all compounds, the NICS(1)<sub>zz</sub> values on the

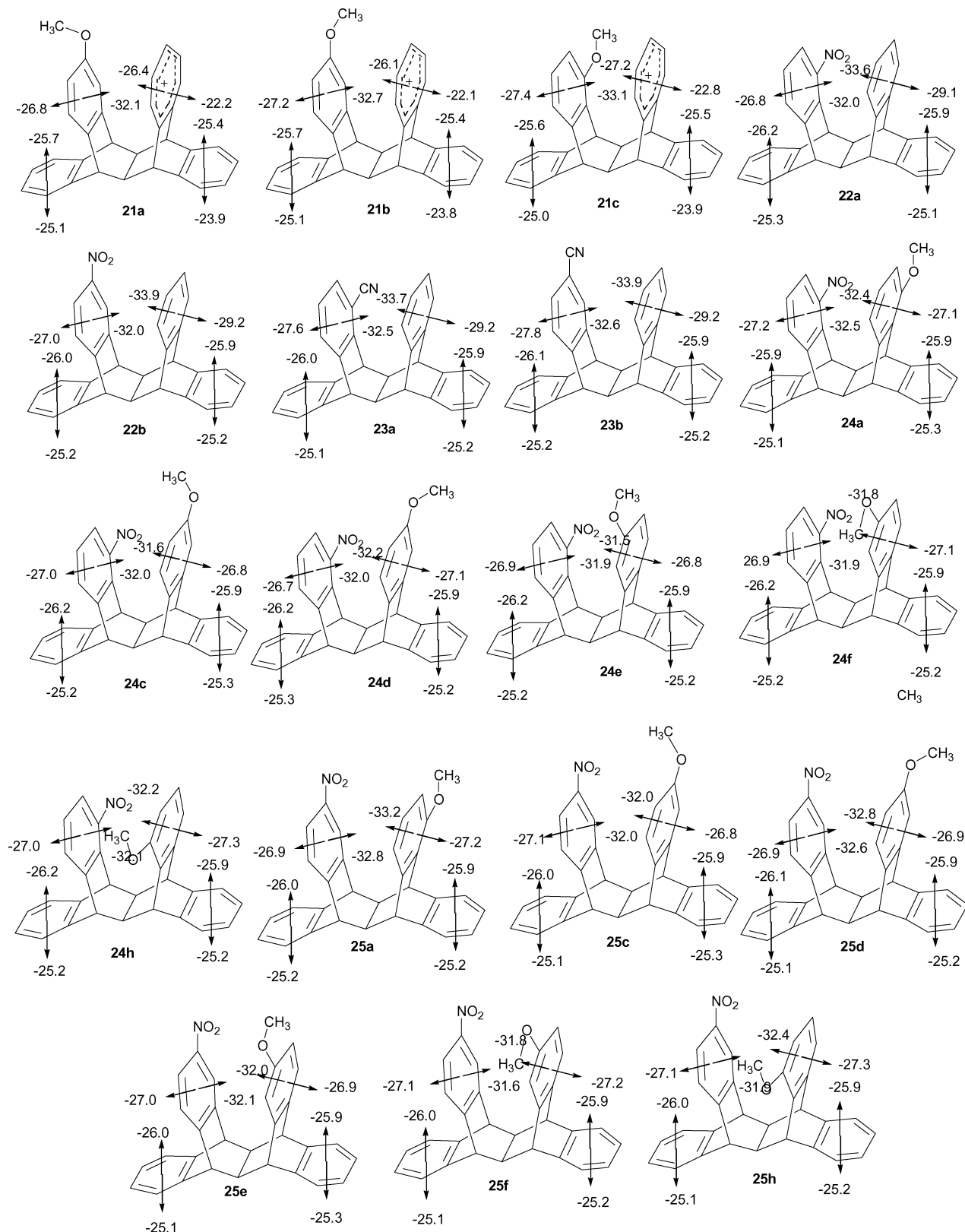
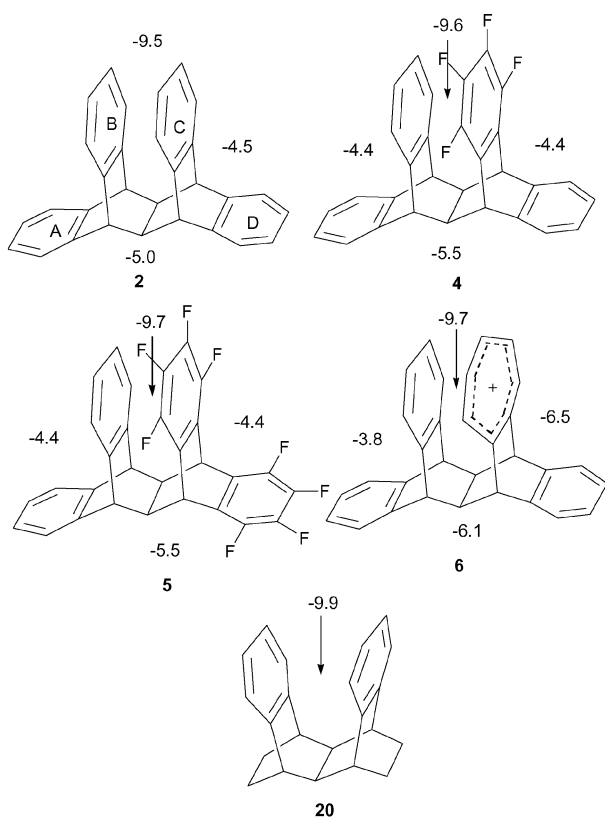


Fig. 11 NICS(1)<sub>zz</sub> for **21a–25h** by B3LYP/6-31G(d).



**Fig. 12** NICS at the average point between ring centers of cofacial rings for **2**, **4–6**, and **20** by B3LYP/6-31G(d).

inside of benzene and tropylium rings are larger than those on the outside. NICS(1)<sub>zz</sub> for **21a–21c** are less negative than those for **6**. In comparison with NICS(1)<sub>zz</sub> values computed for **2**, they are less negative in the substituted benzene rings for **22–25**, but are rather similar for the unsubstituted rings. The NICS(1)<sub>zz</sub> data are rather insensitive to changes in substitution patterns of the methoxy and nitro groups. NICS values at interannular centers (see Fig. 12 and 13) are larger when the interannular distances are smaller. NICS values for **2** are similar to those for **4**, **5**, **20** and no significant substituent effects are manifested. Similar findings were reported on substituent effects by Sola *et al.*<sup>15b</sup> for benzene and for selected heterocyclic aromatics.

For comparison, and as a guide for synthesis, the GIAO-derived <sup>13</sup>C NMR data for these compounds were computed (data summarized in Fig. S12†). Chemical shifts at the unsubstituted ring positions are similar to those in parent **2**. Overall, GIAO data indicate that the <sup>13</sup>C shifts are rather insensitive to variation in transannular π–π interactions in cofacial electron rich/electron poor decks.

#### 5,14;7,12-Bis(*o*-benzeno)-6,13-ethenylidene-5,5a,6,6a,7,12,12a,13,13a,14-decahydropentacene (**8**), related compound **8a**, and their carbocations

Compound **8** (Fig. 14) is a (2:1) Diels–Alder adduct of anthracene and 7-methylenenorbornadiene.<sup>25</sup> Its X-ray structure confirmed the proximity of the double bond with the π-decks.<sup>25</sup> The buried

double-bond did not react in conventional electrophilic addition reactions, but no stable ion studies are as yet undertaken.

Fig. S13† gives a summary of bond-lengths for **8** from X-ray structure<sup>25</sup> versus computed values by B3LYP/6-31G(d). Distances between cofacial decks at the upper part are 7.127–7.248 Å by X-ray and 7.364 Å by DFT calculations. The computed bonds are a little longer, but other bond-lengths are quite similar. There is good overall agreement between the X-ray data and DFT.

Superacid protonation will likely generate an internally π-stabilized carbocation **26** (see Fig. 16). A Wagner–Meerwein rearrangement could potentially lead to a cofacial arenium ion. DFT study of the resulting carbocations (Fig. 14–16), and NICS to examine possible transannular stabilization in the rearranged carbocation provided additional models for the present study which could serve as guide for planned experimental work.

Results of electronic energies (*E*), zero point energies (*ZPE*), and Gibbs free energies (*G*) for 5,14,7,12-bis(*o*-benzeno)-6,13-ethenylidene-5,5a,6,6a,7,12,12a,13,13a,14-decahydropentacene (**8**), related compound **8a**, and their protonated carbocations **26** and **27** (see Fig. 17) are included in Table S2† along with their molecular symmetry. Fig. 17 and 18 show NICS(0), NICS(1) and NICS(1)<sub>zz</sub> data for these structures. For carbocations **26** and **27** increased aromaticity in the interannular space is predicted by NICS(1) and by NICS(1)<sub>zz</sub>. The NICS values are similar between **8** and **8a** and between **26** and **27**.

Fig. S13† provides a summary of the GIAO-derived <sup>13</sup>C NMR data for carbocations **26** and **27**. The carbocation centers in **26** and **27** are at δ 278 and δ 281 ppm respectively, and exhibit similar Δδ<sup>13</sup>Cs relative the their parent hydrocarbons.

According to Butler *et al.*<sup>25</sup> **28** rearranged smoothly into **32**. Structures of compounds shown in Fig. 15 and 16 were calculated by DFT and their energies are summarized in Table S5.† Structures **28**, **29**, **31**, and **32** were found to be minima, but **30** was a transition state (one imaginary frequency by frequency analysis). Hydrocarbon **32** is more stable than **28** by 7.4 kcal (Table S5†) and this agrees with the observed isomerization (**28** → **32**). Carbocation **29** is more stable than **31** by 1.9 kcal mol<sup>-1</sup> and activation Gibbs free energy for **29** → **30** is 11.5 kcal mol<sup>-1</sup>.

On the contrary, **35** is less stable by 6.6 kcal mol<sup>-1</sup> in Gibbs free energy than **8** and carbocation **26** is preferred relative to **34** (Fig. 16, Table S5†). This indicates that compound **8** should not isomerize to **35** under superacid catalysis.

## Summary/Conclusions

We have examined the efficacy of NICS as a probe for sensing the changes in aromaticity due to transannular π–π interactions in rigid cyclophanes and their derived carbocations. The study emphasized the janusene skeleton, its building blocks, and carbocations. It has been shown that NICS(1)<sub>zz</sub> and NICS(1) (albeit to a lesser degree) have the potential to sense/gauge variations in aromaticity resulting from transannular π–π interactions in these systems, and could therefore be utilized alongside experimental approaches (NMR, UV, and chemistry) and other theoretical approaches (HOMO–LUMO forms and energy gaps) for studying transannular aromaticity in rigid cyclophanes. These methods did not, however, prove sensitive enough for reliable sensing of through-space substituent effects.

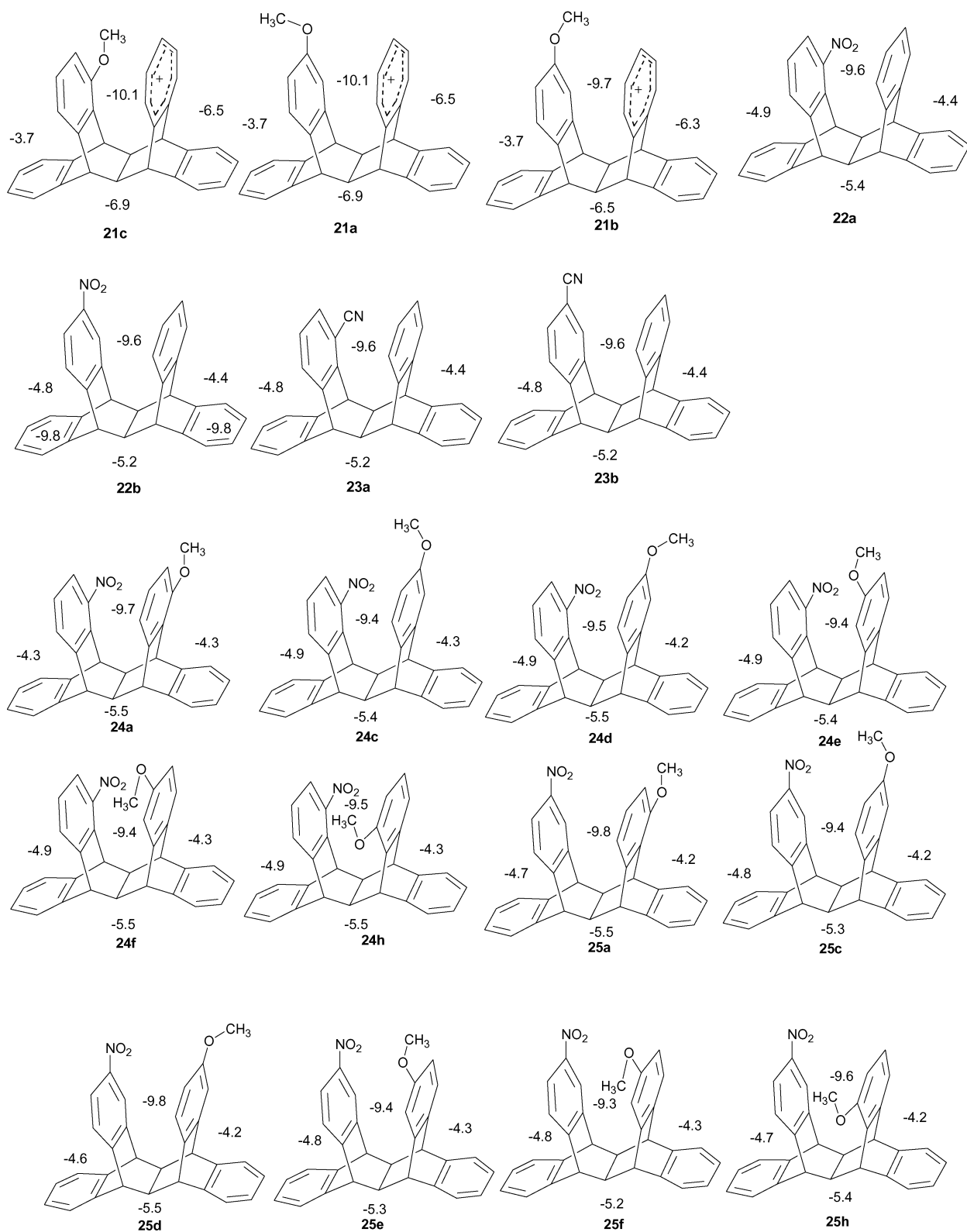


**Fig. 13** NICS at the average point between ring centers of cofacial rings for **21a–25h** by B3LYP/6-31G(d).



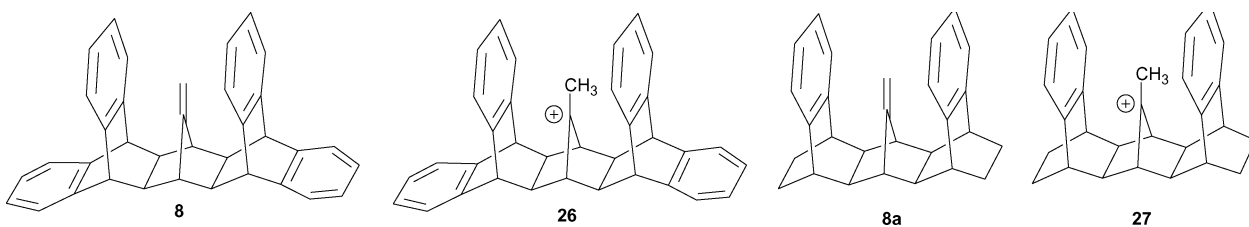


**Fig. 14** 5,14;7,12-Bis(*o*-benzeno)-6,13-ethenylidene-5,5a,6,6a,7,12,12a,13,13a,14-decahydropentacene (**8**), related compound **8a**, and their carbocations **26** and **27**.

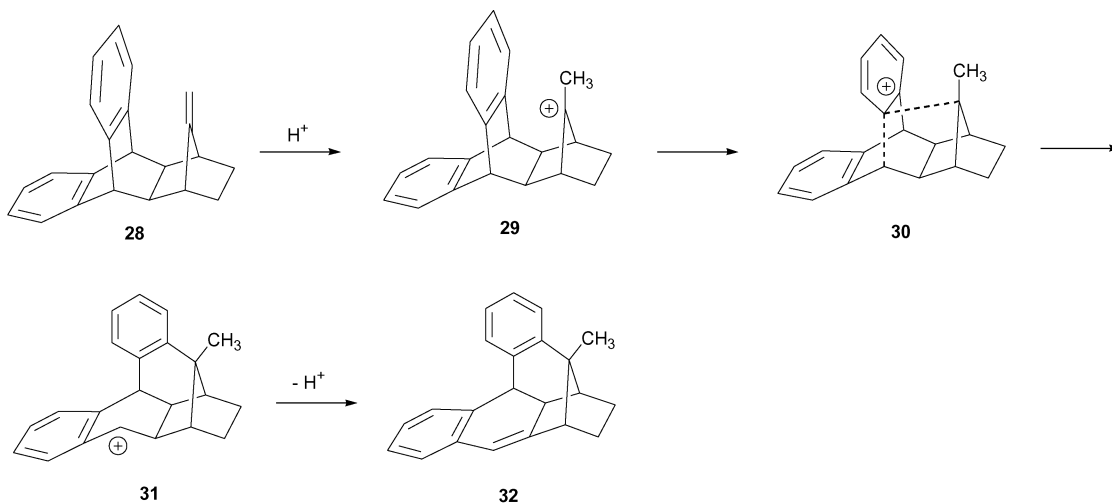


**Fig. 15** Rearrangement of **28** to **32** via carbocations **29** and **31**.

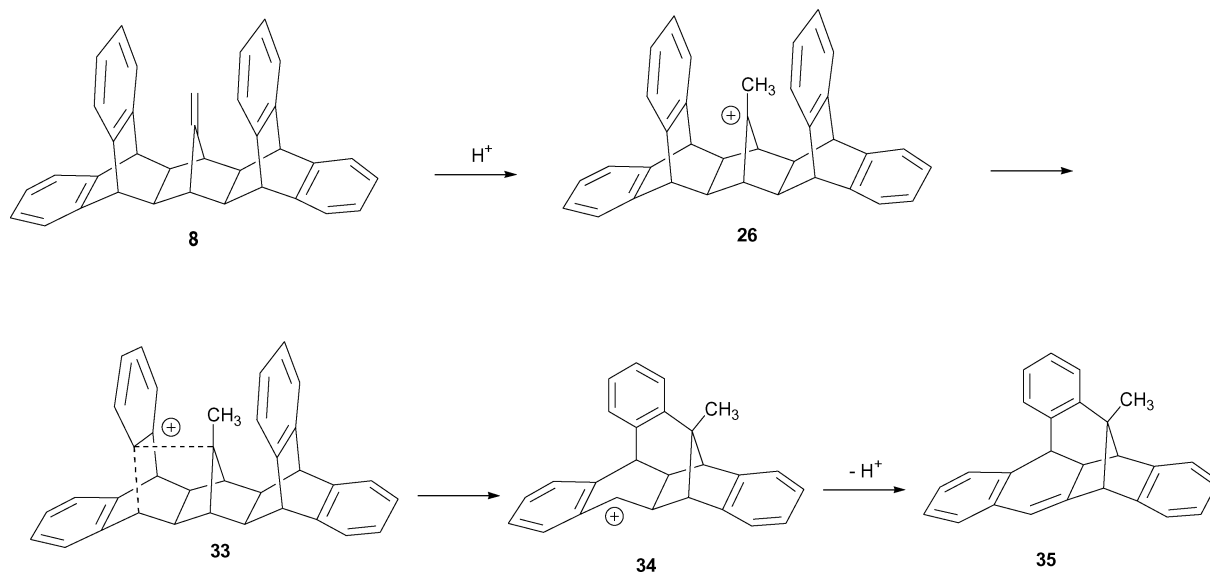


**Fig. 16** Improbable rearrangement from **8** to **35** via carbocations **26** and **34**.

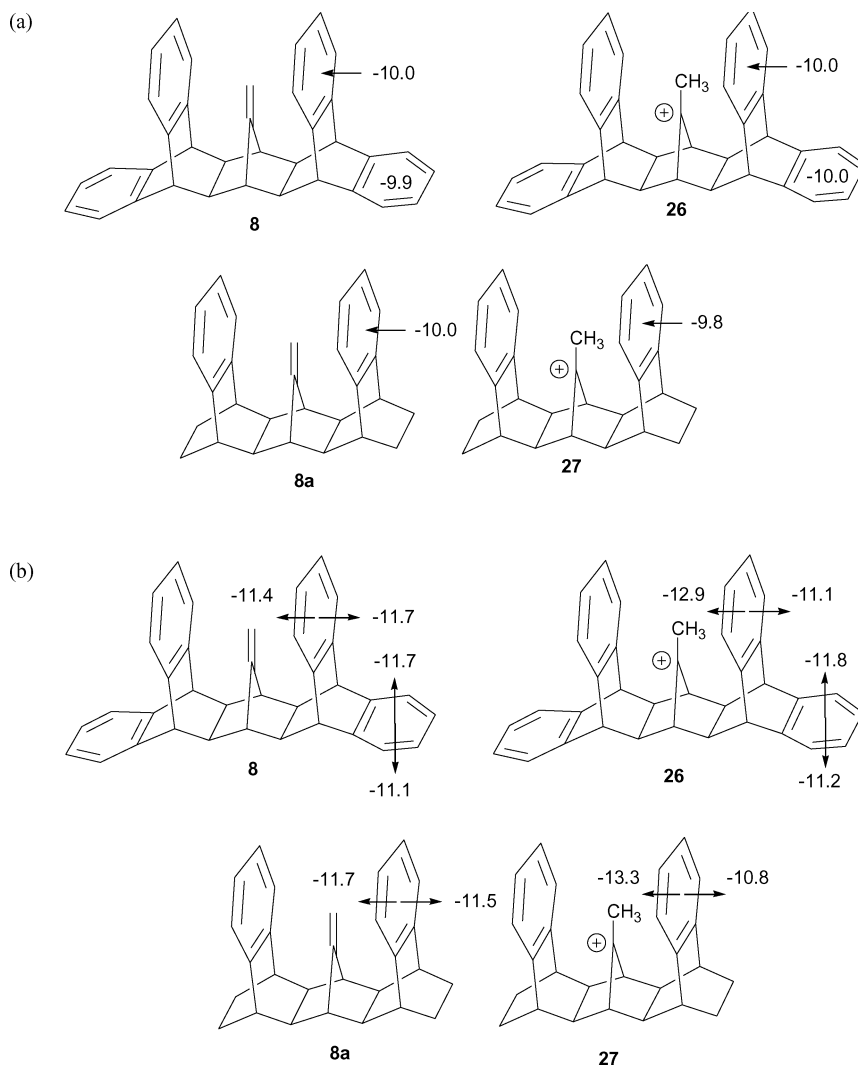


Fig. 17 a. NICS(0) for **8**, **8a**, **26** and **27** by B3LYP/6-31G(d), b. NICS(1) for **8**, **8a**, **26** and **27** by B3LYP/6-31G(d).

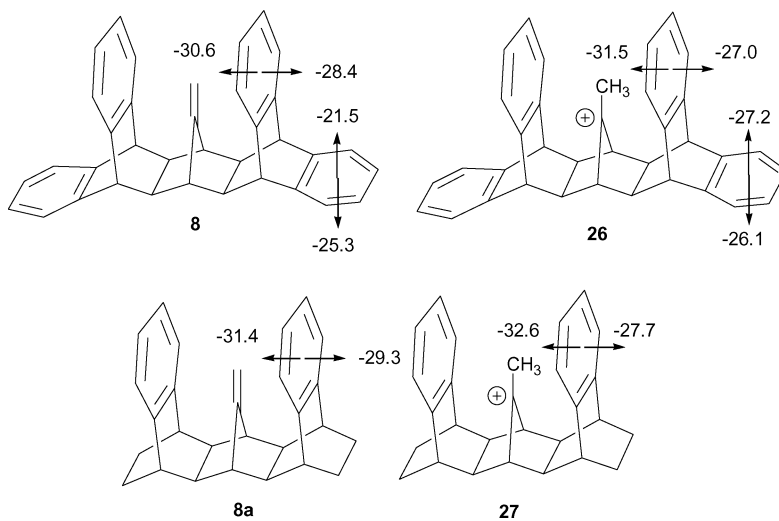


Fig. 18 NICS(1)<sub>zz</sub> for **8**, **8a**, **26** and **27** by B3LYP/6-31G(d).

## References

- 1 P. v. R. Schleyer, C. Maerker, A. Dransfeld, H. Jiao and N. J. R. van Eikema Hommes, *J. Am. Chem. Soc.*, 1996, **118**, 6317–6318.
- 2 (a) C. S. Wannere, K. W. Sattelmeyer, H. F. Schaefer, III and P. v. R. Schleyer, *Angew. Chem., Int. Ed.*, 2004, **43**, 4200–4206; (b) I. Alkorta, I. Rozas and J. Elguero, *Tetrahedron*, 2001, **57**, 6043–6049.
- 3 (a) W. Collier, S. Saebø and C. U. Pittman, Jr., *THEOCHEM*, 2001, **549**, 1–8; (b) S. M. Bachrach, *J. Organomet. Chem.*, 2002, **643–644**, 39–46; (c) A. Matinez, M.-V. Vazquez, J. L. Carreon-Macedo, L. E. Sansores and R. Salcedo, *Tetrahedron*, 2003, **59**, 6415–6422.
- 4 P. v. R. Schleyer, B. Kiran, D. V. Simion and T. S. Sorensen, *J. Am. Chem. Soc.*, 2000, **122**, 510–513.
- 5 D. Moran, M. Manoharan, T. Heine and P. v. R. Schleyer, *Org. Lett.*, 2003, **5**, 23–26.
- 6 (a) B. Reindl, T. Clark and P. v. R. Schleyer, *J. Phys. Chem. A*, 1998, **102**, 8953–8963; (b) I. Morao and I. H. Hillier, *Tetrahedron Lett.*, 2001, **42**, 4429–4431.
- 7 (a) T. Okazaki and K. K. Laali, *Org. Biomol. Chem.*, 2004, **2**, 2214–2219; (b) T. Okazaki and K. K. Laali, *J. Org. Chem.*, 2004, **69**, 510–516; (c) K. K. Laali, T. Okazaki and S. E. Galembeck, *J. Chem. Soc., Perkin Trans. 2*, 2002, 621–629; (d) T. Okazaki and K. K. Laali, *Org. Biomol. Chem.*, 2005, **3**, 286–294; (e) T. Okazaki and K. K. Laali, *Org. Biomol. Chem.*, 2003, **1**, 3078–3093.
- 8 (a) N. S. Mills, *J. Am. Chem. Soc.*, 1999, **121**, 11690–11696; (b) N. S. Mills, *J. Org. Chem.*, 2002, **67**, 7029–7036; (c) A. Levy, A. Rakowitz and N. S. Mills, *J. Org. Chem.*, 2003, **68**, 3990–3998.
- 9 (a) F. Stahl, P. v. R. Schleyer, H. Jiao, H. F. Schaefer, III, K.-H. Chen and N. L. Allinger, *J. Org. Chem.*, 2002, **67**, 6599–6611; (b) I. Alkorta, J. Elguero, M. Eckert-Maksic and Z. B. Maksic, *Tetrahedron*, 2004, **60**, 2259–2265; (c) C. Dardonville, M. L. Jimeno, I. Alkorta and J. Elguero, *Org. Biomol. Chem.*, 2004, **2**, 1587–1591.
- 10 (a) P. v. R. Schleyer, M. Manoharan, H. Jiao and F. Stahl, *Org. Lett.*, 2001, **3**, 3643–3646; (b) J.-I. Aihara and H. Kanno, *J. Phys. Chem. A*, 2005, **109**, 3717–3721; (c) G. Portella, J. Poater and M. Sola, *J. Phys. Org. Chem.*, 2005, **18**, 785–791.
- 11 J.-I. Aihara, *Bull. Chem. Soc. Jpn.*, 2003, **76**, 103–105.
- 12 (a) D. Sawicka and K. N. Houk, *J. Mol. Model.*, 2000, **6**, 158–165; (b) D. Sawicka, Y. Li and K. N. Houk, *J. Chem. Soc., Perkin Trans. 2*, 1999, 2349–2355.
- 13 P. v. R. Schleyer, M. Manoharan, Z.-X. Wang, B. Kiran, H. Jiao, R. Puchta and N. J. R. van Eikema Hommes, *Org. Lett.*, 2001, **3**, 2465–2468.
- 14 C. Corminboeuf, T. Heine, G. Seifert, P. v. R. Schleyer and J. Weber, *Phys. Chem. Chem. Phys.*, 2004, **6**, 273–276.
- 15 (a) G. Portella, J. Poater, J. M. Bofill, P. Alemany and M. Sola, *J. Org. Chem.*, 2005, **70**, 2509–2521; (b) J. Poater, M. Duran, M. Sola and B. Silvi, *Chem. Rev.*, 2005, **105**, 3911–3947.
- 16 G. F. Caramori, S. E. Galembeck and K. K. Laali, *J. Org. Chem.*, 2005, **70**, 3242–3250.
- 17 R. Salcedo, N. Mireles and L. E. Sansores, *J. Theor. Comput. Chem.*, 2003, **2**, 171–177.
- 18 N. Mireles, R. Salcedo, L. E. Sansores and A. Martinez, *Int. J. Quantum Chem.*, 2000, **80**, 258–263.
- 19 (a) K. Laali and R. Filler, *J. Fluorine Chem.*, 1989, **43**, 415–427 and earlier references cited therein; (b) K. K. Laali, E. Gelerinter and R. Filler, *J. Fluorine Chem.*, 1991, **53**, 107–126, and earlier reports cited therein; (c) K. K. Laali, J. J. Houser, R. Filler and Z. Kong, *J. Phys. Org. Chem.*, 1994, **7**, 105–115; (d) K. K. Laali and D. A. Forsyth, *J. Org. Chem.*, 1993, **58**, 4673–4680.
- 20 Review: D. J. Cram and J. M. Cram, *Acc. Chem. Res.*, 1971, **4**, 204–213.
- 21 K. Wolfram and M. C. Holthausen, *A Chemist's Guide to Density Functional Theory*, Wiley-VCH: Weinheim, 2nd edn., 2000, Chapter 11.
- 22 M. J. Frisch, G. W. Trucks, H. B. Schlegel, G. E. Scuseria, M. A. Robb, J. R. Cheeseman, J. A. Montgomery, Jr., T. Vreven, K. N. Kudin, J. C. Burant, J. M. Millam, S. S. Iyengar, J. Tomasi, V. Barone, B. Mennucci, M. Cossi, G. Scalmani, N. Rega, G. A. Petersson, H. Nakatsuji, M. Hada, M. Ehara, K. Toyota, R. Fukuda, J. Hasegawa, M. Ishida, T. Nakajima, Y. Honda, O. Kitao, H. Nakai, M. Klene, X. Li, J. E. Knox, H. P. Hratchian, J. B. Cross, C. Adamo, J. Jaramillo, R. Gomperts, R. E. Stratmann, O. Yazyev, A. J. Austin, R. Cammi, C. Pomelli, J. W. Ochterski, P. Y. Ayala, K. Morokuma, G. A. Voth, P. Salvador, J. J. Dannenberg, V. G. Zakrzewski, S. Dapprich, A. D. Daniels, M. C. Strain, O. Farkas, D. K. Malick, A. D. Rabuck, K. Raghavachari, J. B. Foresman, J. V. Ortiz, Q. Cui, A. G. Baboul, S. Clifford, J. Cioslowski, B. B. Stefanov, G. Liu, A. Liashenko, P. Piskorz, I. Komaromi, R. L. Martin, D. J. Fox, T. Keith, M. A. Al-Laham, C. Y. Peng, A. Nanayakkara, M. Challacombe, P. M. W. Gill, B. Johnson, W. Chen, M. W. Wong, C. Gonzalez and J. A. Pople, *Gaussian 03, Revision B.05*, Gaussian, Inc., Pittsburgh PA, 2003.
- 23 K. Wolinski, J. F. Hinton and P. Pulay, *J. Am. Chem. Soc.*, 1990, **112**, 8251–8260; R. Ditchfield, *Mol. Phys.*, 1974, **27**, 789–807.
- 24 R. F. W. Bader and C. Chang, *J. Phys. Chem.*, 1989, **93**, 5097–5107 and related references cited therein.
- 25 D. N. Butler, I. Gupta, W. W. Ng and S. C. Nyburg, *J. Chem. Soc., Chem. Commun.*, 1980, 596–597.
- 26 Z. Chen, C. S. Wannere, C. Corminboeuf, R. Puchta and P. v. R. Schleyer, *Chem. Rev.*, 2005, **105**, 3842.